Polish Journal of Environmental Studies Vol. 12, No. 5 (2003), 619-627

Seasonal Variation in the Chemical Composition and Morphology of Aerosol Particles in the Centre of Katowice, Poland

A. Wawroś[1]*, E.Talik[1], M. Żelechower[2], J. S. Pastuszka[3], D. Skrzypek[1], Z. Ujma[1]

[1]August Chełkowski Institute of Physics, University of Silesia, 4 Uniwersytecka St., 40-007 Katowice, Poland.
[2]Department of Materials Science, Silesian University of Technology, 8 Krasińskiego St., 40-019 Katowice, Poland.
[3]Institute of Occupational Medicine & Environmental Health, 13 Kościelna St., 41-200 Sosnowiec, Poland.

Received: 30 January, 2003
Accepted: 27 March, 2003

Abstract

PM-2.5 and PM-10 samples were collected in the centre of Katowice, Poland during February to May 2001. They were analyzed by gravimetry, X-ray photoelectron spectroscopy and scanning electron microscopy combined with an energy dispersive spectrometer and electron paramagnetic resonance. The combination of these methods allows us to analyze elemental composition, size and morphology of more than three hundred individual atmospheric particles.

The composition of the aerosol particles is strongly influenced by meteorological conditions such as wind speed and direction. Mineral elements mainly existed in large-size particles. The anthropogenic pollution elements, however, are contained in corpuscles (< 2 μm). In comparison with the situation in the wintertime, the number of particles rich in some heavy metals in springtime was found to be lower. The EPR spectra are complex and their features correspond to: I type: Cu^{2+} centra in a low-symmetry host site, II type: radical species in the soot, which appears as the paramagnetic pyrolyzed product.

Keywords: aerosols, SEM-EDS, XPS, EPR

Introduction

The aerosol samples collected from November 1995 to October 1996 in the towns of Świętochłowice, Pszczyna and Kielce were analyzed recently using the XPS method [1]. These investigations were performed within the international program CESAR/PHARE. Particles of an aerodynamic diameter less than 2.5 μm (PM-2.5) and less than 10 μm (PM-10) were collected using the Harvard impactors. Our results showed significant differences in the structure of atmospheric aerosol particles in the urban areas of southern Poland, indicating that these particles are of various origins. Also the optical properties of the aerosol particles are different in these towns. The most absorptive aerosols were found in the towns located in Upper Silesia [2]. Currently, atmospheric aerosol studies using the XPS method are continued in the centre of Katowice.

Katowice, the capital of Upper Silesia, is located in middle southern Poland. Upper Silesia belongs to the most populated area in Poland and even the most polluted regions of the world. The existence of heavy industry and road traffic is the main source of anthropogenic particles, which dominate in this region. Detailed knowledge of aerosol composition and meteorological conditions is useful for identification and localisation of the polluters. Pollution characteristics and especially aerosol particles depend on the season. Microscopic analysis indicated that there are mainly aluminosilicates together with iron and

*Corresponding author; e-mail: ola@kulpa.zfcst.us.edu.pl

Table 1. Mass concentration of atmospheric aerosol in the centre of Katowice and wind characteristics.

Sampling day	Concentration [μg/m^3]				Wind speed [m/s]	Wind direction
	PM – 2.5		PM - 10			
	I	II	I	II		
February 8/9	27	35	50	53	3.6	S
February 21/22	22	23	33	27	5.8	W
March 9/10	90	-	104	102	2.9	S
March 21/22	56	58	64	71	2.3	E
April 5/6	101	114	118	143	2.2	N, W, S
April 19/20	51	54	58	72	1.7	N, W
May 10 /11	16	15	29	34	1.8	N
May 23/24	21	22	45	47	2.2	N, E, W

I - Sampling point located on the roof of the Institute of Physics; II - Sampling point located on the roof of the canteen of University

titanium oxides, as well as calcium sulphates, calcium carbonates and sodium chlorides during the winter season. The crustal elements Al, Si and Ca were significantly dominant not only to the coarse fraction but also to the fine fraction. A mixture of aluminosilicate particles with iron oxides and compounds of barium was also observed. The presence of barite nanocrystals in the Upper Silesia aerosol is the result of burning Ba-enriched coals [3]. Some particles had a typical morphological structure as wurtzite and gallium arsenide. The particles collected in the winter period close to the main road can be determined as copper chlorine, chromium compounds, wurzite, iron oxide (combine with some rare earth elements, such as La, Ce and Nd), aluminosilicates with iron oxides and enriched in lead. Even fine particles contain heavy metals such as copper, zinc, chromium, iron, lead and nickel [4]. These heavy metals can be toxic due to their biochemical activity [5].

This paper describes the elemental composition and morphology of the aerosol particles collected in the centre of Katowice in the period of February-May using XPS technique, scanning electron microscopy combined with energy dispersive spectrometer and EPR in relation to meteorological data.

Methods

Sampling

24-hours concentrations of PM-10 and PM-2.5 were sampled in the period from February to May 2000 with a frequency of two consecutive days several times a month (Table 1). Two sampling points were situated in the centre of Katowice (at a height of 25 m above ground level on the roof of the Institute of Physics) and near a busy road (at a height 10 m above ground level on the roof of the University canteen). The aerosol samples were collected using Harvard impactors. The Harvard impactors (Air Diagnostics and Engineering Inc., Naples, Maine, USA), designed to sample the PM-10 and PM-2.5 fractions, were equipped with the pump units designed and built by the Wageningen Agricultural University (The Netherlands). The flow rate was 10 l/min. The airborne particles were collected on type SC, Millipore 8.0 μm pore size filters, 2 μm pore size Teflon filters and subsequently subjected to gravimetric analyses.

Photoelectron Measurements

The XPS spectra of aerosol samples were obtained using a PHI 5700/660 Physical Electronics Photoelectron Spectrometer with monochromatized Al K_α X-ray radiation (1486.6 eV). The hemispherical mirror analyser analyzed the energy of the electrons with an energy resolution of about 0.3 eV. X-ray emission from a surface area of 800 x 2000 μm was measured. Analysis time for the investigated aerosol samples was 12 h to obtain good statistics. All measurements were performed under UHV conditions, 10^{-10} Torr. In every case the neutraliser was used due to a charge effect which occurs for non-conducting samples. The binding energy was determined by reference to the C 1s component set at 284.8 eV. Each peak of the recorded spectrum is characteristic for a certain electron energy level of a certain element. The electron binding energies are characteristic for each element. However, in compounds the binding energies are not absolutely constant but depend on the chemical environments due to modification of the valence electron distribution. These differences in relation to pure elements in the electron binding energies are called chemical shifts. The identification of the compounds was done using the catalogue of the chemical shifts [6]. For many XPS investigations it is important to determine the relative concentrations of the various constituents. The

Table 2. Composition [at. %] of the particulate atmospheric aerosol determined by XPS method.

I – Sampling point located on the roof of the Institute of Physics

Element [at. %]		8/9.02.01		21/22.02.01		9/10.03.01		21/22.03.01		5/6.04.01		19/20.04.01		10/11.05.01		23/24.05.01	
		PM 2.5	PM 10	PM 2.5	PM 10	PM 2.5	PM 10	PM 2.5	PM 10	PM 2.5	PM 10	PM 2.5	PM 10	PM 2.5	PM 10	PM 2.5	PM 10
C 1s	sample	73.80	71.31	57.99	55.81	71.19	73.75	61.26	59.58	76.22	74.07	62.71	53.88	34.79	36.88	49.25	51.63
	filter	3.69	3.69	10.00	14.46	5.85	3.23	6.77	10.92	2.31	3.85	8.61	13.69	11.12	12.61	5.57	4.27
O 1s	sample	15.72	17.37	21.67	14.97	14.92	15.81	21.75	16.88	15.05	13.84	17.32	17.74	6.47	10.22	10.15	13.84
	filter	2.18	2.18	5.91	8.54	3.45	1.91	4.00	6.45	1.36	2.27	5.09	8.09	-	-	-	-
N 1s	sample	2.35	2.23	2.18	1.97	2.57	2.61	3.50	2.93	2.57	2.21	3.02	2.93	0.73	0.88	1.38	1.35
	filter	0.24	0.24	0.65	0.94	0.38	0.21	0.44	0.71	0.15	0.25	0.56	0.89	-	-	-	-
F 1s	sample	-	0.01	-	-	-	-	-	-	-	-	-	-	45.95	31.17	32.03	25.62
	filter	-	-	-	-	-	-	-	-	-	-	-	-	-	-	-	-
S 2p		1.01	1.08	0.46	0.84	0.82	0.85	1.40	1.11	0.81	0.93	1.03	0.93	0.31	0.41	0.80	0.92
Si 2p		0.17	0.53	0.56	0.47	0.20	0.51	0.13	0.33	0.28	0.62	0.18	0.23	0.15	0.76	0.21	0.65
Cl 2p		0.13	0.21	0.10	0.60	0.10	0.20	0.03	0.16	0.62	0.67	0.32	0.41	0.03	0.11	0.04	0.21
Na 1s		0.40	0.49	0.22	0.61	0.32	0.29	0.37	0.28	0.27	0.44	0.54	0.31	0.12	0.18	0.25	0.36
Zn $2p_{1/2}$		0.08	0.08	0.15	0.26	0.05	0.06	0.13	0.12	0.23	0.23	0.38	0.45	0.12	0.16	0.07	0.09
Al 2s		0.05	0.18	0.04	0.11	0.03	0.17	0.02	0.08	-	0.19	-	0.08	0.12	0.19	0.05	0.24
Cu 2p		0.01	0.01	-	0.01	-	0.01	0.02	0.01	-	-	0.01	0.01	-	-	0.01	0.01
Fe 2p		0.02	0.04	0.01	0.09	-	0.06	0.03	0.05	0.01	0.11	0.09	0.09	-	-	-	0.03
Ca 2p		0.01	0.13	0.01	0.06	-	0.10	0.02	0.17	-	0.11	0.02	0.15	0.02	0.35	0.07	0.47
K 2s		0.13	0.15	0.02	0.10	0.09	0.18	0.07	0.10	0.08	0.15	0.07	0.05	0.05	0.06	0.12	0.15
Mg 1s		0.01	0.05	0.02	0.13	0.01	0.04	0.01	0.05	0.01	0.05	0.01	0.02	-	0.01	-	0.11
Pb 4f		0.01	0.01	-	-	-	-	0.01	0.01	0.01	0.01	0.02	0.01	0.01	0.01	-	0.01
I $3d_{5/2}$		-	-	0.01	0.01	0.01	0.01	-	0.01	0.01	-	-	0.01	-	-	-	0.01
Ti 2p		-	-	-	-	0.01	-	0.01	-	-	-	-	0.01	-	-	-	-
P 2p		-	0.02	-	0.01	-	0.01	-	-	-	-	-	-	-	-	-	0.01
Cr $2p_{3/2}$		-	-	-	-	-	-	-	0.04	-	-	-	0.01	-	0.03	-	0.01

II – Sampling point located on the roof of the canteen.

Element [at. %]		8/9.02.01		21/22.02.01		9/10.03.01	21/22.03.01		5/6.04.01		19/20.04.01		10/11.05.01		23/24.05.01	
		PM 2.5	PM 10	PM 2.5	PM 10	PM 10	PM 2.5	PM 10	PM 2.5	PM 10	PM 2.5	PM 10	PM 2.5	PM 10	PM 2.5	PM 10
C 1s	sample	72.11	68.90	58.21	58.22	69.78	64.69	59.72	77.41	77.36	62.89	63.60	38.69	41.97	49.68	51.88
	filter	2.77	5.08	10.77	9.69	3.23	6.31	8.77	2.62	1.70	9.23	9.08	11.62	13.17	7.50	5.04
O 1s	sample	18.42	17.18	19.69	20.63	18.96	19.89	19.50	13.68	15.52	17.10	15.94	6.92	8.63	11.36	13.13
	filter	1.64	3.00	6.36	5.73	1.91	3.73	5.18	1.55	1.00	5.45	5.36	-	-	-	-
N 1s	sample	2.74	2.40	2.18	2.12	3.14	2.94	2.94	2.41	1.77	2.47	2.46	0.69	0.67	1.50	1.24
	filter	0.18	0.33	0.70	0.63	0.21	0.41	0.57	0.17	0.11	0.60	0.59	-	-	-	-

Table 2 continues on next page...

F 1s	sample	-	-	-	0.01	-	0.01	0.02	-	-	-	-	41.25	33.99	27.86	25.17
	filter	-	-	-	-	-	-	-	-	-	-	-	-	-	-	-
S 2p		1.16	1.10	0.71	0.68	1.04	1.27	1.33	0.97	0.75	0.88	1.00	0.39	0.38	1.50	0.93
Si 2p		0.14	0.59	0.40	0.61	0.51	0.22	0.54	0.39	0.48	0.21	0.48	0.11	0.39	1.03	0.76
Cl 2p		0.08	0.17	0.21	0.42	0.19	0.03	0.18	0.22	0.31	0.24	0.27	0.03	0.13	0.29	0.16
Na 1s		0.46	0.47	0.40	0.55	0.33	0.26	0.36	0.24	0.47	0.25	0.30	0.07	0.09	0.05	0.42
Zn $2p_{1/2}$		0.07	0.07	0.17	0.20	0.08	0.04	0.16	0.11	0.08	0.44	0.37	0.11	0.20	0.32	0.08
Al 2s		0.04	0.20	0.04	0.12	0.19	0.07	0.25	0.05	0.15	0.02	0.20	0.04	0.14	0.04	0.28
Cu 2p		0.01	0.01	0.01	0.01	0.01	0.01	0.02	0.01	0.01	0.01	0.04	0.01	-	0.05	0.01
Fe 2p		0.02	0.16	-	0.06	0.09	0.02	0.07	0.03	0.11	0.05	0.12	-	-	0.01	-
Ca 2p		0.01	0.12	0.01	0.07	0.09	0.02	0.21	0.02	0.07	-	0.09	0.01	0.15	-	0.39
K 2s		0.13	0.14	0.06	0.08	0.19	0.06	0.11	0.08	0.07	0.06	0.06	0.04	0.05	0.06	0.39
Mg 1s		0.02	0.05	0.07	0.17	0.04	-	0.03	0.03	0.03	0.04	0.03	-	0.02	0.21	0.09
Pb 4f		0.01	0.01	0.01	-	-	0.01	0.01	0.01	-	0.01	0.02	0.01	0.01	0.03	-
I $3d_{5/2}$		-	0.01	-	-	0.01	0.01	-	0.01	-	-	0.01	-	-	-	0.01
Ti 2p		-	-	-	-	-	-	-	-	-	-	-	-	-	-	-
P 2p		-	0.02	-	-	-	-	0.02	-	0.01	-	-	-	-	-	-

Multipak Physical Electronics program enables quantification of the XPS spectra utilising peak area and peak height sensitivity factor. Calculation of the standard atomic concentration provides a ratio of each component to the sum of the other taken into account elements in the data. Considered are only those elements for which the specific line is clearly visible in the spectrum. For those lines the background is subtracted, the limit of the region of the line is individually set, after which integration is done [6].

SEM Observations and Electron Probe X-Ray Microanalysis

The aerosol samples were coated in vacuum with a film of carbon in order to dissipate the electrical charge formed during SEM observations and electron probe X-ray microanalysis. A carbon coating has been chosen despite high carbon mass absorption coefficients (for low Z elements) because other possible coating elements (Al, Ti, Cr and Cu) could be present in aerosol. The morphological characterisation of the aerosol was established by the scanning electron microscope JSM35 combined with the LINK 860 energy dispersive spectrometer (Si-Li detector, beryllium window, and analytical range from Na to U). During SEM observation and X-ray microanalysis an accelerating voltage of 25 kV and a beam current of 2×10^{-10} A were applied. These experimental conditions have been selected to obtain high X-ray count rates and good quality of SEM micrographs. Although the examined aerosol is composed mainly of light elements, some heavy elements may be present (for instance lead, zinc), and the minimum recommended overvoltage ratio $U = E_0/E_{K(L)}$ should equal at least 2 in order to obtain reasonable characteristic X-ray line intensities (i.e. Pb-L series or even Zn-K series). Here, E_0 denotes the primary electron beam energy and $E_{K(L)}$ critical excitation energy of the K or L series. Quantitative analysis of separate particles was not performed for reasons mentioned below, but spectra from some pure sulphates (of ammonium, calcium, magnesium and sodium) have been measured in order to compare them qualitatively to the spectra of some particles contained in aerosol.

Electron Paramagnetic Resonance

The X-band (ν = 9 GHz) EPR spectra in 160–350 K range were recorded on a standard Radiopan spectrometer with double modulation of magnetic field of a frequency of 100 kHz.

Results and Discussion

PM-2.5 and PM-10 mass concentrations and meteorological conditions measured from February to May for two sampling sites, in the centre of Katowice, are reported in Table 1. It can be found that the average concentration of PM-10 was 63 $\mu g/m^3$ and 69 $\mu g/m^3$ in sampling points I

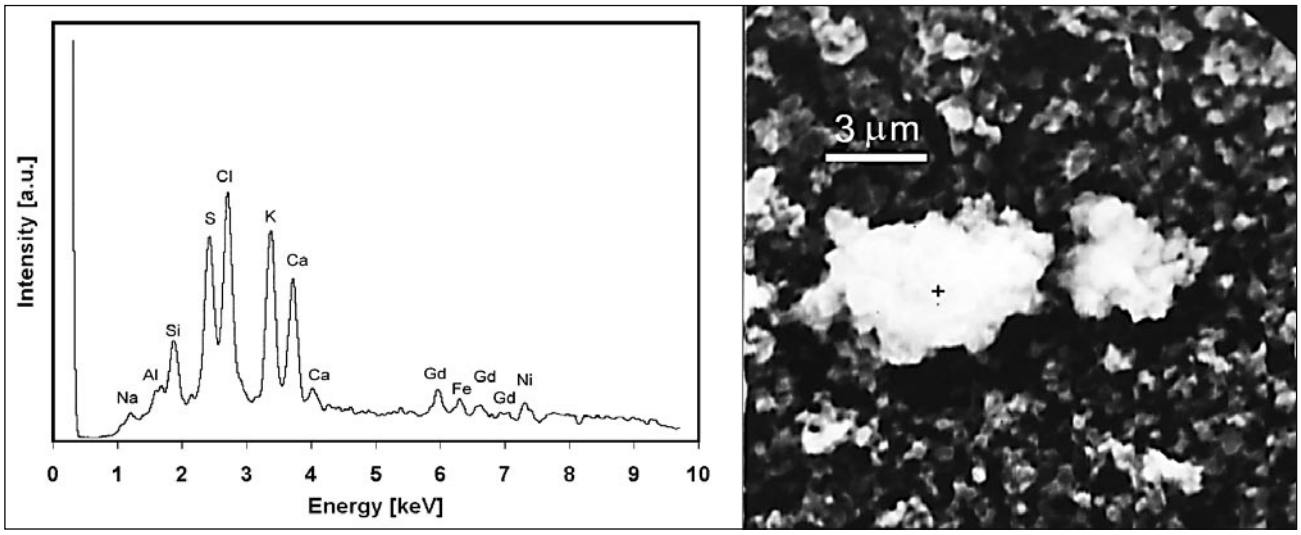

Fig. 1. Particle of complex mixture. X-ray spectrum and corresponding SEM micrograph. Beryllium window detector.

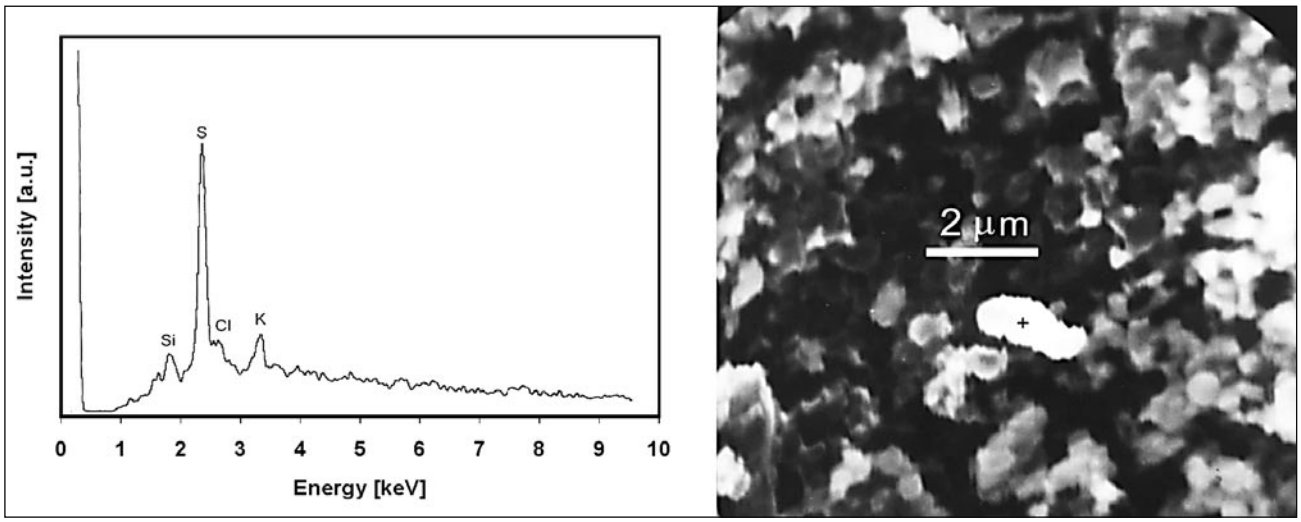

Fig. 2. Sulphur-rich particle. X-ray spectrum and corresponding SEM micrograph. Beryllium window detector.

and II, respectively. Also, the average concentration level of fine particles (PM-2.5) was slightly higher in site II (46 μg/m^3) than in site I (42 μg/m^3 – excluding the data obtained in March 9/10 for better comparison), which indicates the influence of traffic on atmospheric aerosol during the study period.

The XPS analysis of the aerosol samples was performed for a wide range of elements such as C, O, N, F, Fe, Si, S, Na, Zn, I, Cu, Cl, Al, Ca, Mg, Pb, P, Ti, K and Cr (Table 2). The elements C, O, N and F were detected also in blank filters. Some elements were present in every case (e.g. C, O, S, Si, Zn, Cl and Na) and some were specified for sampling point located on the roof of the Institute of Physics (Cr and Ti).

The microscopic investigations were taken to provide information on shape, size, surface and other properties of more than three hundred individual atmospheric particles. The obtained results show the significant differences in the morphology and chemical composition of aerosol particles collected in the centre of Katowice during the period February-May. Examples of electron micrographs of individual airborne particles are shown in Figures 1-4 together with the X-ray spectra of these particles (beryllium window detector). Points of qualitative analyses are marked with black crosses (Figures 1-4). Aluminosilicates predominate in February and are assigned to both natural and anthropogenic origin. Aluminosilicates with spherical shapes come from anthropogenic sources, in contrast to irregularly shaped particles that are classified as natural (soil) particles. Most of them were agglomerates consisting of smaller particles and enriched by such heavy metals as Fe, Ni, Cu, Zn and rare earth as Gd. Figure 1 shows an example of the detection results. Rare earth elements are rather uncommon, but recent application of them is

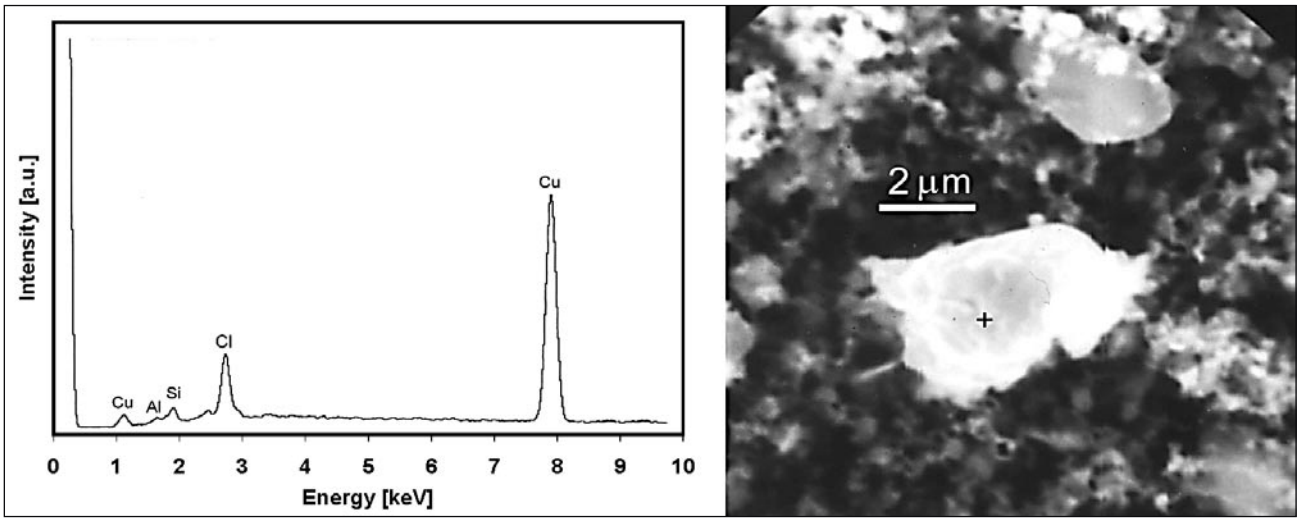

Fig. 3. Particle of copper chloride (CuCl). X-ray spectrum and corresponding SEM micrograph. Beryllium window detector.

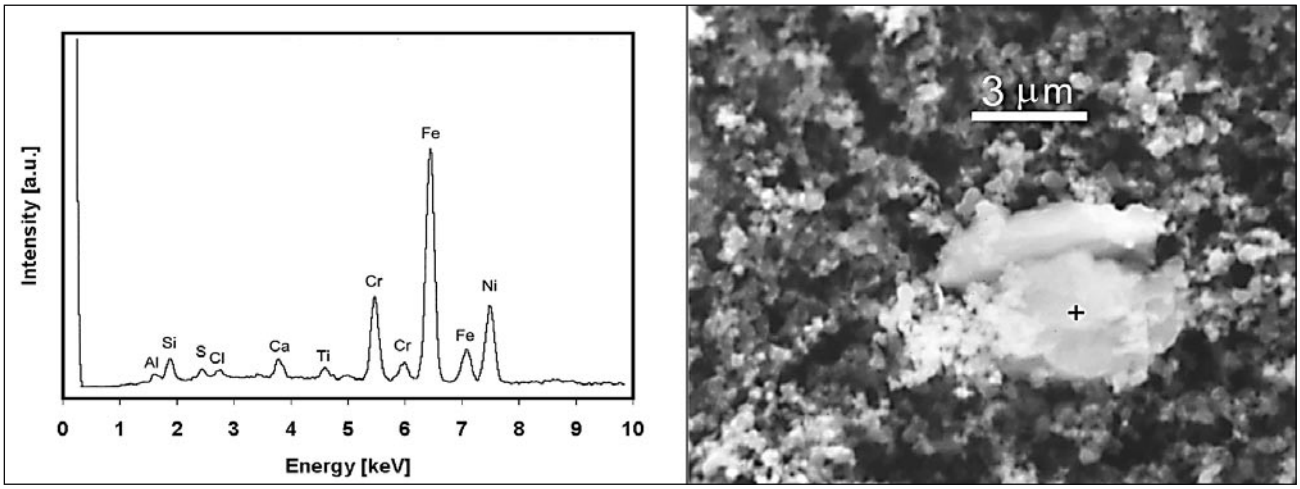

Fig. 4. Particle rich in heavy metals. X-ray spectrum and corresponding SEM micrograph. Beryllium window detector.

increasing. Rare earth elements are used in pigments for paint and plastics, substituting heavy metal pigments (e.g. lead and cadmium), in catalytic converters for diesel engines and in automobile windscreen wiper motors [7]. Due to the nearness of the sampling points to the main road and significant building construction place the particles contained rare earth elements were detected. Similar particles contained rare earths, and heavy metals were observed in a few samples collected in December [4]. Moreover, the big particles recognized as calcium sulphates and calcium carbonates were found. The size of these particles varies between 4.5 and 20 µm. Elemental composition of aerosol particles collected from March to May was very similar. The results showed that the aerosol consists mainly of smaller particles, which were identified as aluminosilicates with titanium, magnesium, iron and nickel. A great number of the S-rich particles, in the form of needles with diameters above 1 µm, were observed. Such S-rich particles are very often described in literature [8, 9]. They may originate from sulphates formed from gaseous SO_2 or by biomass burning. The particles coming from biomass burning are additionally enriched in potassium. In most of our investigated S-rich particles a small amount of potassium and/or sodium was found (Fig. 2). Also several CuCl particles were found (Fig. 3). Silica oxides in the spherical form, aluminosilicates, NaCl and particles rich in potassium were mostly observed for bigger size fractions (10-20 µm). Biological particles were found in the majority of samples in the spring period. These particles were classified on the basis of their chemical composition and/or characteristic morphology [10].

Additionally, in May some particles rich in such heavy metals as Ti, Cr, Fe, Zn and Ni were also found. A typical particle is shown (Fig. 4). Anthropogenic particles containing Ni are the products of diesel and residual oil burning [11]. Almost all Fe-rich particles are oxides and occur as spheres with diameters less than 2 µm. Probably, the presence of iron in the fine particles is derived from

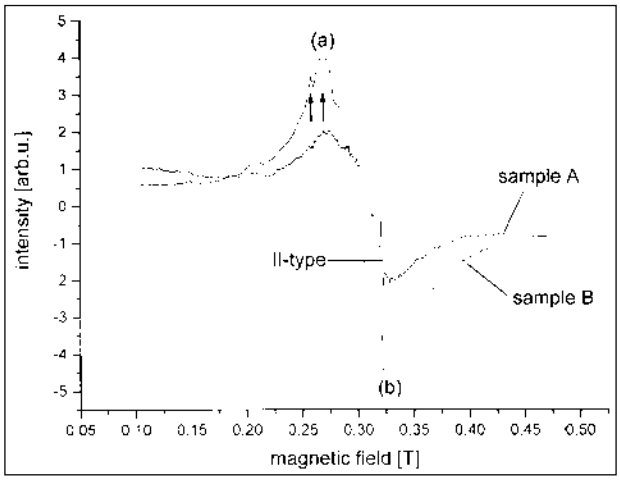

Fig. 5. The X-band EPR spectra of sample A and sample B at ambient temperature.

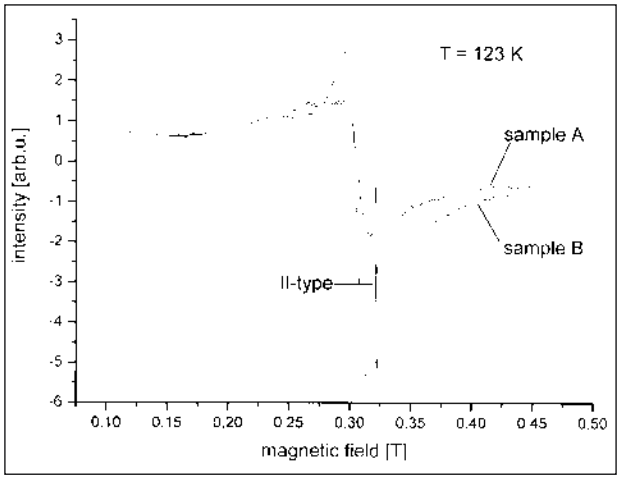

Fig. 6. The representative EPR spectra of aerosols recorded at low temperature.

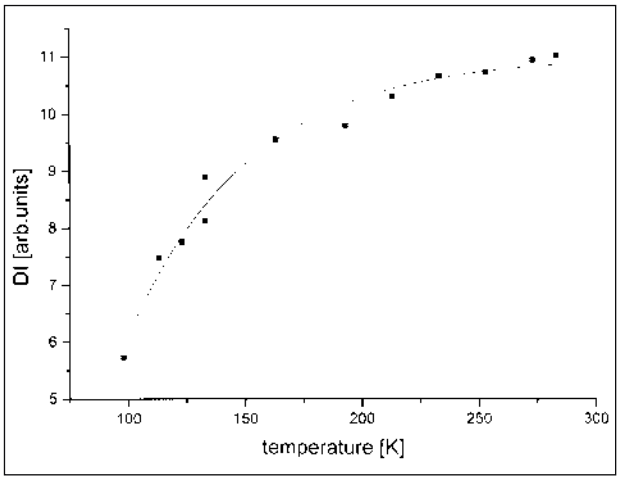

Fig. 7. Plot of signal intensity vs. temperature for the sample B (the full line is a guide to the eye).

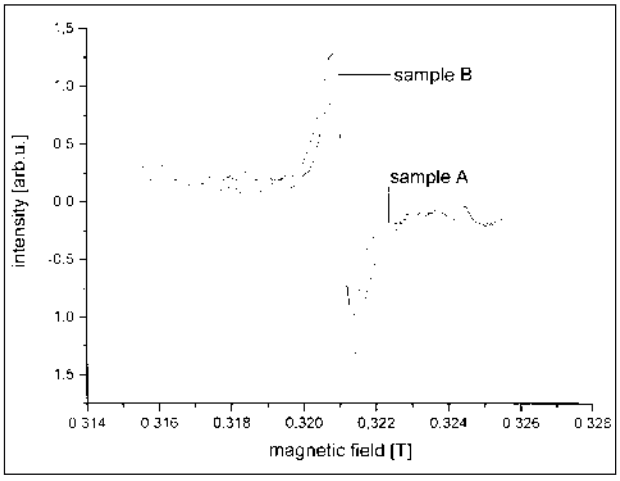

Fig. 8. EPR spectra corresponding to the soot.

combustion sources like refuse and oil [12, 13]. Tires and motor oils are commonly considered as a major source of Zn from road traffic [14-16].

The atmospheric aerosols are characterised by using electron paramagnetic resonance technique. The EPR spectra of atmospheric fine (sample A) and coarse particles (sample B) are shown in Fig. 5. Two types of EPR signals were observed:

type I - the broad line centred at $g_{eff} = 2.050$ (sample A) and $g_{eff} = 2.110$ (sample B)

type II - the narrow signal with $g = 2.0025$

The EPR spectra from two sampling points in the centre of Katowice were tested. The results show no difference in EPR parameters such as g-factor (g) and linewidth (ΔB). However, as it was expected, the intensity of the EPR signal (estimated as the double integrated EPR signal (DI)) is different for materials collected on filter 2.5 and 10. The ratio of DI (B) to DI (A) is 2.95 for I-type signal and 1.48 for II-type signal, respectively. The representative spectra recorded in low temperature are shown in Fig. 6.

Type I EPR Spectra

EPR spectrometry has applicability to paramagnetic transition metal ions and our attention was focused on iron and copper ions. The EPR spectra of aerosols as EPR spectra of transition metal ions in disordered materials are interpreted. The EPR spectra in disordered materials are characterized by broad distributions of the magnetic parameters such as g-factor and D and A-tensors. A common feature of these spectra is the broadness of their absorption lines.

The iron can appear as ferric Fe^{3+} or ferrous Fe^{2+} ions. The five d-electron state of Fe^{3+} can exist in two configurations as the high-spin (HS, S = 5/2) and low-spin (LS, S = ½) forms, respectively. The EPR spectrum of Fe^{3+} in a disordered system consists of lines at $g_{eff} = 4.3$ and

$g_{eff} = 2$. The presence of the $g_{eff} = 4.3$ feature characterizes the EPR spectrum of Fe^{3+}. It is absent in our spectra. The ferrous ions also have two configurations - low-spin with S = 0 and high-spin with S = 2. The Fe^{2+} ions are "EPR silent" not only in the LS-diamagnetic state, but usually in the HS-paramagnetic state, as well (at least at ambient temperature and in microwave bands) because of very rapid spin-lattice relaxation processes and/or large zero-field splitting. Therefore, its presence can be detected by EPR only in an indirect way. Usually, the EPR spectrum is modified in the course of the presence of Fe^{2+} (HS) ions. Note that there can be two different ways of this modification. Firstly, broadening of EPR linewidth leads to a disappearnce of spectra. Secondly, by unusual temperature dependence of EPR linewidth [17].

In the whole temperature range, from 100 K to 350 K, we observed a superposition of an anisotropic and more isotropic EPR spectra. These spectra show a marked g-factor anisotropy and a poor resolved hyperfine structure. We believe that the spectra originated from copper (II) ions. The divalent copper ion state ^2D of the configuration $3d^9$ is an orbital quintet (L = 2) and its ground state is characterized by spin S = ″. The spin Hamiltonian for the Cu^{2+} ion with orthorhombic distortion is given by:

$$H = \mu_B g_{\parallel} B_z S_z + \mu_B g_{\perp} (B_x S_x + B_y S_y) + A_{\parallel} I_z S_z + A_{\perp} (I_x S_x + I_y S_y)$$

Where g and A are the g-tensor and the hyperfine structure tensor, respectively.

The hyperfine structure originated from the copper nucleus whose spin I = 3/2 (for both Cu^{63} and Cu^{65} isotopes). Two sets marked as (a) and (b) in Fig. 5 may be respectively designated as parallel and perpendicular hyperfine peaks. The perpendicular hyperfine peaks are resolved barely with "10" filter but not at all with "2.5" filter.

Cantin et al. [18] studied a polymer compound by EPR, using Cu^{2+} as dopants and paramagnetic probes. At liquid nitrogen temperature typical anisotropic spectra of Cu^{2+} in a static Jahn-Teller configuration were observed, while the room temperature spectra undergo dynamic averaging. The coexistence of anisotropic and motionally averaged EPR spectra was explained in terms of a model based on a statistical distribution of the energy difference between the lowest and the two higher potential energy minima of the Jahn-Teller centre in a low-symmetry host site. We believe that this model can be applied to a description of investigated materials. It is difficult to determine an accurate value of magnetic parameters, because aerosols are the amorphous solids. The feature of the EPR spectra in such materials is distribution of spin-Hamiltonian parameters around mean values and the broadness of their absorption lines. This is associated with the randomness of the glass structure. Simultaneously, the width of the parallel hyperfine peaks of amorphous solids increases rapidly from peak to peak in order of m (the magnetic quantum number of copper nucleus). This resulted in worse resolution of the hyperfine structure. The approximate value of $A_{\parallel}$ was estimated from the positions of two sharper peaks signed by arrows on the spectrum (see Fig. 5).

sample A: $g_{\parallel} = 2.248$; $g_{\perp} = 2.101$;

sample B: $g_{\parallel} = 2.256$; $g_{\perp} = 2.118$; $|A_{\parallel}| = 118 \cdot 10^4 cm^{-1}$;

An anomalous decrease of the double integrated EPR signal (DI) was observed upon lowering the temperature (Fig. 7). This temperature dependence has no trivial explanation within the framework of conventional EPR theory. We suggest that the origin of this behaviour may be attributed to:

a) the temperature dependent non-resonant surface absorption,
b) the presence of separated antiferromagnetic clusters.

II Type EPR Spectra

During the last decade numerous epidemiological studies of association between respiratory diseases and air pollution were performed. Special attention was paid to toxic free radicals.

The narrow sharp singlet line (line II in Fig. 5) is shown in Fig. 8. This spectrum corresponds to the soot appearing as the paramagnetic pyrolyzed product. Its EPR parameters are g = 2.0025 and $\Delta B = 0.64$ mT at room temperature. Recently the same spectrum was investigated by Yordanov et al. [19] in details. Their paper presents the applicability of EPR spectrometry for separate estimation of soot and polycyclic aromatic hydrocarbons present in aerosols.

Conclusions

The seasonal variation in chemical composition and morphology of aerosol particles collected in the centre of Katowice was presented. Based on our measurements and analyses the following conclusions can be given.

Most of the particles were soil erosion particles from earth materials. Calcium was the predominant element in the coarse particles. Also, aluminosilicates and iron-rich particles were commonly rounded and probably come from coal combustion. Compared to the situation in the winter season, the number of particles containing heavy metals such as chromium, lead and manganese generally decrease during the spring season. In the majority of cases, these particles derived from industrial sources.

EPR spectra are complex and their features correspond to:

type I: Cu^{2+} centra in a low-symmetry host site and type II: radical species in the soot which appear as free radicals of pyrolyzed product.

Acknowledgements

We would like to thank Dr. Lesław Ośródka and Mr. Krystian Rorbek (The Meteorological Institute, Katowice Branch) for their help in obtaining and analyzing the meteorological data.

References

1. WAWROŚ A., TALIK E., PASTUSZKA J.S. Investigation of aerosols from Świętochłowice, Pszczyna and Kielce by XPS method. J. Alloys Comp. **328**, 171, **2001**.
2. PASTUSZKA J.S., WAWROŚ A., TALIK E., PAW U K.T. Optical and chemical characteristics of the atmospheric aerosol in four towns in southern Poland. Sci. Total Environ., submitted.
3. JABŁOŃSKA M., RIETMEIJER F.J.M., JANECZEK J. Fine-grained barite in coal fly ash from the Upper Silesia Industrial Region. Environ. Geol. **40**, 941, **2001**.
4. WAWROŚ A., TALIK E., PASTUSZKA J.S. Investigation of winter atmospheric aerosol particles in downtown Katowice using XPS and SEM. Microsc. Microanal., submitted.
5. LIGHTY J.S., VERANTH J.M., SAROFIM A.F. Combustion aerosols: factors governing their size and composition and implications to human health. J. Air Waste Manage. Assoc. **50**, 1565, **2000**.
6. MOULDER J.F., STICKLE W.F., SOBOL P.E., BOMBEN K.D. Handbook of X-ray Photoelectron Spectroscopy Physical Electronics, **1995**.
7. SMART J.V. Rare Earths. Mineral Information Leaflet No2. Department of Mines and Energy, The State of Queensland, **1999**. http:/www.nrm.gld.gov.au/mines/rarearth.pdf
8. ZHANG D., IWASAKA Y., BAI Y., SHI G. Aerosol particles around Lhasa City, Tibet, China, in summer 1988: Individual particle analysis. J. Aerosol Sci. **31** (Suppl. 1), 319, **2000**.
9. SOBANSKA S., COEUR C., PAUWELS B., MAENHAUT W., ADAMS F. Micro-characterisation of tropospheric aerosols from the Negev Desert, Israel. J. Aerosol Sci. **31** (Suppl. 1), 344, **2000**.
10. EBERT M., WEINBRUCH S., HOFFMANN P., ORTNER H.M. Chemical characterisation of North Sea aerosol particles. J. Aerosol Sci. **33**, 613, **2000**.
11. MIRANDA R.M., ANDRADE M.F., WOROBIEC A., GRIEKEN R.V. Characterisation of aerosol particles in São Paulo Metropolitan. Area. Atmos. Environ. **36**, 345, **2002**.
12. ANDRADE F., ORSINI C., MAENHAUT W. Relation between aerosol source and meteorological parameters for inhalable atmospheric particles in São Paulo City, Brazil. Atmos. Environ. **28**, 2307, **1994**.
13. SEINFELD J.H., PANDISS.N. Atmospheric chemistry and physics from air pollution to climate change. Wiley, New York, **1998**.
14. PIERSON W.R., BRACHACZEK W.W. Particulate matter associated with vehicles on the road. II. Aerosol Sci. Technol. **2**, 1, **1983**.
15. HUANG X, OLMEZ I., ARAS K., GORDON G.E. Emission of trace elements from motor vehicles: potential marker elements and source composition profile. Atmos. Environ. **28**, 1385, **1994**.
16. SÖRME L., BERGBÄCK B., LOHM U. Goods in the anthroposphere as a metal emissions source - a case study of Stockholm, Sweden. Water, Air, and Soil Pollut. **1**, 213, **2001**.
17. BIAŁAS-BORGIEŁ K., SKRZYPEK D., ZIPPER E. The effect of paramagnetic impurities on EPR linewidth in $KMnF_3$. Experimental and theoretical studies. J. Phys. C **13**, 6251, **1980**.
18. CANTIN C., DAUBRIC H., KLIAVA J., KAHN O. Coexistence of anisotropic and motionally averaged EPR spectra in a Jahn-Teller system: Cu^{2+} ion in $[Fe(NH_2trz)_3(NO_3)]_2$ compound Sol. St. Comm. **108**, 17, **1998**.
19. YORDANOV N.D., LUBENOVA S., SOKOLOVA S. On the possibility for separate determination of pyrolyzed products (soot and polycyclic aromatic hydrocarbons) in aerosols by EPR spectrometry. Atmos. Environ. **35**, 827, **2001**.